

A High Gain Observer for Enclosed Mass Estimation in a Spark Ignited Engine

Maria Adelina Rivas Caicedo, Emmanuel Witrant, Olivier Sename and Pascal Higelin

Abstract—A high gain non linear observer is implemented to estimate the enclosed mass in the combustion chamber of a spark ignited engine. The observer uses the cylinder pressure measurement during the compression and combustion strokes to estimate the enclosed mass. An engine model is proposed and used as a virtual engine to build the observer. The model is validated by comparison with real measurements, obtained from experimental tests. The results of the observer are compared with the virtual engine model.

I. INTRODUCTION

The estimation of the total mass enclosed in the combustion chamber is an interesting and challenging task for the engine control community. An accurate estimation of the cylinder enclosed mass would permit a better control of the associated fuel injection and a better treatment of the pollutants residuals. The introduction of more complicated features such as variable valve timing (VVT), cam profile switching and variable geometry intake manifold in new production engines require more advanced techniques to estimate the cylinder enclosed mass [1]. When including these features, one of the most common phenomenon is the appearance of back flows. This phenomenon combined with possible mass scavenging might induce a difference between the actual mass and the measurement provided by the mass flow meter in the intake manifold.

In automotive control, the variables in the air path are typically used to compute the cylinder characteristics, such as the in-cylinder load and residual mass fraction, (e.g. see [2], [3], [4] and [5]). In this work, the objective is to estimate the total enclosed mass in the combustion chamber during the compression and combustion strokes. This mass corresponds to the total air load plus the residual mass. If the total enclosed mass in the combustion chamber is accurately estimated, the air load can be computed by subtracting the residual mass from the total enclosed mass. Strategies as the ones proposed in [5] and [6] might be used to compute the residual mass.

A considerable number of open loop techniques have been proposed recently to compute the total enclosed mass. Examples of this modeling technique are described

in [7], [5] and [4]. In those models, a balance between the total mass in the cylinder at the inlet valve closure (IVC), the back flow and the trapped mass at exhaust valve closure (EVC) are taken into account. Following the open loop strategy, iterative approaches that use the cylinder pressure measurement during the compression and combustion strokes have also been proposed. For instance, iterative methods to compute the enclosed mass during the compression stroke are proposed in [8], [6] and [9].

Alternatively, closed loop observer schemes have also been developed to estimate the engine load during the admission stroke, thus constraining the estimated variables with the online measurement. In [10], the uncertainties of the measurements in the intake manifold are introduced and an adaptative learning algorithm is used to track the error between the measured pressure and the estimation. In [11], a periodic observer for a class of non-linear models in the discrete Takagi-Sugeno form is designed, using the variables on the engine intake manifold. Both works propose suitable methods for computing the enclosed mass in the combustion chamber, by computing the in-cylinder mass in the intake manifold before the valves closure.

The aim of this paper is to present an estimation method for the total mass of all the species in the compression and combustion strokes, during the valves closure, using the cylinder pressure measurement. This strategy does not need many engine cycle computations to achieve the mass estimation. A high gain non linear observer of the cylinder temperature during the valves closure is built and the enclosed mass is computed using the observed temperature and the cylinder pressure measurement.

This paper is structured as follows: in Section II, a physical model of the engine used as a virtual engine is presented. A reduced model for the compression and combustion strokes when the valves are closed is developed in Section III. In Section IV the reduced model is transformed into an equivalent system in additive triangular form, where the high gain observer is implemented: the cylinder enclosed mass is computed in this stage. Simulations of the observed variables are compared with the validated virtual engine to support the results of the observer.

Maria Adelina Rivas Caicedo, Emmanuel Witrant and Olivier Sename are with UJF, INPG, CNRS, *ENSE³*, 11 rue de mathématiques, BP 46, 38402 Saint Martin d'Hères Cedex, France. (maria-adelina.rivas-caicedo, emmanuel.witrant, olivier.sename)@gipsa-lab.fr

Pascal Higelin is with PRISME, Polytech'Orleans, Site Vinci JOULE 112, 8 Rue Leonardo Da Vinci, 45072 Orleans Cedex, France. pascal.higelin@univ-orleans.fr

II. SYSTEM MODELING

The 0D engine model proposed in [12] is implemented and used as virtual engine. This model provides, among others, the cylinder pressure, the cylinder temperature, the clearance volume and the mass dynamics. The whole engine cycle is captured by this model.

The cylinder pressure dynamics is:

$$\begin{aligned} dp(t) = & \frac{r}{V(t)c_v}Q_{h_{in}}(t) - \frac{r}{V(t)c_v}Q_{h_{out}}(t) \\ & - \frac{r}{V(t)c_v}p(t)dV(t) - \frac{p(t)dV(t)}{V(t)} \\ & + \frac{r}{V(t)c_v}LHVQ_{m_{comb}}(t) \\ & - \frac{r}{V(t)c_v}Q_{th}(t) \end{aligned} \quad (1)$$

and the cylinder temperature dynamics is:

$$\begin{aligned} dT(t) = & \frac{1}{m(t)c_v} \left(-p(t)dV(t) - Q_{th}(t) + (Q_{h_{in}}(t) \right. \\ & \left. - Q_{h_{out}}(t) + LHVQ_{m_{comb}}) - T(t)c_v dm(t) \right) \end{aligned} \quad (2)$$

where $p(t)$ is the cylinder pressure, $T(t)$ is the cylinder temperature and $V(t)$ is the gas volume. $Q_{h_{in}}$ and $Q_{h_{out}}$ represent the enthalpy flow between the inlet and outlet ports of the system, respectively, and $dm(t)$ is the mass balance in the combustion chamber. r is the ideal gas constant and c_v is the specific heat at constant volume. The wall losses Q_{th} are expressed as:

$$Q_{th}(t) = h_c(t)A_w(t)(T(t) - T_w) \quad (3)$$

where $A_w(t)$ is the wall transfer area, $T(t) - T_w(t)$ is the temperature difference between the gases and the cylinder walls, and $h_c(t)$ is the heat transfer coefficient computed from Woschni's empirical law [13]:

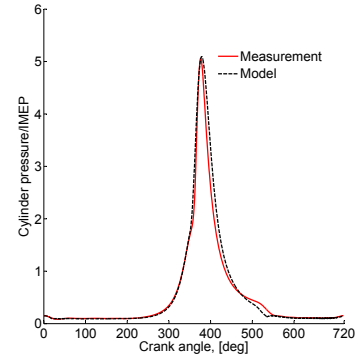
$$\begin{aligned} h_c(t) = & \alpha D^{-0.2} p(t)^{0.8} T(t)^{-0.53} \left(C_1 V_p + \right. \\ & \left. C_2 \frac{V_s T_1}{p_1 V_1} (p(t) - p_0(t)) \right) \end{aligned} \quad (4)$$

where D is the cylinder bore, C_1 and C_2 are calibration constants, p_1 and T_1 represent the known state of the working gas related to the instantaneous cylinder volume V_1 , i.e. at *IVC*, and p_0 is the pressure reference in the absence of combustion. $LHVQ_{m_{comb}}(t)$ is the enthalpy supplied by the combustion process. LHV is the lower heat value: for gasoline engines it is approximately $4.15 \times 10^7 \text{ M J k g}^{-1}$ and $Q_{m_{comb}}$ is the burning rate which is commonly defined with a burned mass fraction curve provided by a Wiebe's law [14]:

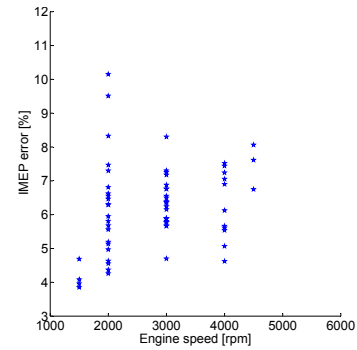
$$\begin{aligned} Q_{m_{comb}}(\theta, u) = & m_o a e^{-a \left(\frac{\theta}{\Delta\theta} \right)^{(m_w+1)}} \\ & \cdot (m_w + 1) \left(\frac{\theta}{\Delta\theta} \right)^{m_w} \frac{2N\pi}{60\Delta\theta} \end{aligned} \quad (5)$$

where N is the engine speed in *rev/s*, m_o is the injected fuel and a , m_w and $\Delta\theta$ are calibration parameters.

The engine model is tested taking as reference the measurements of a 1.2 liters spark ignited engine, characterized by a four-valve chamber. The data to fit the model is the cylinder pressure. The results shown in Figure 1a correspond to a test performed at $N = 1200 \text{ rpm}$ and $\text{IMEP} = 10.68 \text{ bar}$, the cylinder pressure curves are normalized with respect to the IMEP. In the Figures, the measurement is presented in solid lines and the model in dashed lines.



(a) Cylinder pressure. IMEP=10.68 bar, N=1200 rpm.



(b) IMEP error with respect to the engine speed

Fig. 1: Model validation results

The model error is validated by computing the absolute value of the difference between the mean effective pressure (IMEP) of the model and the IMEP measurement. This difference is transformed to percentage with respect to the IMEP measurement. In Figure 1b the model error with respect to the engine speed is depicted. The system has less than 10% of error using this criterion. Those results are accurate enough for the purpose of this work because the aim is not to provide an engine model but to illustrate a

methodology to estimate the wall losses when the valves are closed. More complex modeling strategies can be consulted in [15], where a two zones thermodynamical model with flame wall interaction has been proposed.

III. MODEL REDUCTION

A reduced model for the compression and combustion strokes when the valves are closed is proposed in this section.

During the valves closure, the unique energy components are the enthalpy due to the combustion Q_{hcomb} , the wall losses Q_{th} and the work delivered by the piston. The enthalpy due to the valves flows $Q_{h_{in/out}}$ is zero. Thus from (1) and (2) (changing the notation by $x_1 = p$ and $x_2 = T$), the dynamics of the system during the valves closure is (the time dependence is omitted from this point to simplify the notations):

$$\begin{aligned} \dot{x}_1 &= -\left(\frac{r}{c_v} + 1\right) \frac{dV}{V} x_1 - \frac{r}{c_v V} \delta Q_{th} + \frac{r}{c_v V} Q_{hcomb} \\ \dot{x}_2 &= \frac{rx_2}{Vc_v x_1} \left(-x_1 dV - \delta Q_w + Q_{hcomb} \right) \\ y &= x_1, \quad u = IT \end{aligned} \quad (6)$$

where the system input u is the ignition timing and the measured output y is the cylinder pressure x_1 . The wall losses Q_{th} are first modeled using Wochni's approximation in (4). Even if this approximation is widely used in 0D engine modeling, it contains strong nonlinearities that are hard to handle from the observation point of view. For this reason, a reduced model for the compression and combustion strokes of the wall losses has been created. The proposed approximation keeps the convection principle from (3) but replaces the convection coefficient h_c for a simpler structure:

$$h_c = \omega_e x_1 \quad (7)$$

Similarly to Wochni's principle, the new Q_{th} proposal assumes that the convection coefficient is proportional to the engine speed and the cylinder pressure and two calibration parameters k_1 and k_0 are introduced. Thus, the engine wall losses are computed as:

$$Q_{th} = A_w \omega_e x_1 (k_1 x_2 - k_0 T_w) \quad (8)$$

The wall losses model reduction is calibrated with respect to Wochni's approximation and a satisfactory result is obtained. The reduced model of the wall losses is also included in the 0D virtual engine model with good results. In Figure 2a, two examples for different operation conditions of the validation of the wall losses reduction model are presented. The relative error between equations (3) and (8) is plotted in Figure 2b. The error was computed as the norm of the

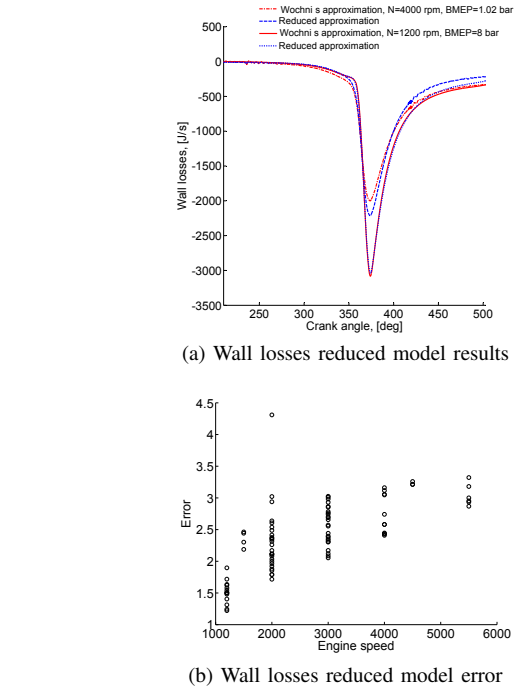


Fig. 2: Wall losses reduced model results

models difference divided by the reference maximum.

Including the reduced wall losses model and grouping the system parameters as:

$$\begin{aligned} a_1 &= -\left(\frac{r}{c_v} + 1\right) \frac{dV}{V}, \quad a_2 = -\frac{r}{c_v V} \\ a_3 &= -\frac{rdV}{c_v V}, \quad a_4 = -\frac{r}{c_v V} A_w \omega_e \end{aligned} \quad (9)$$

system (6) yields

$$\begin{aligned} \dot{x}_1 &= a_1 x_1 + a_4 x_1 (k_1 x_2 - k_0 T_w) - a_2 Q_{hcomb} \\ \dot{x}_2 &= a_3 x_2 + a_4 x_2 (k_1 x_2 - k_0 T_w) - a_2 \frac{x_2}{x_1} Q_{hcomb} \end{aligned} \quad (10)$$

The enclosed mass is then estimated using the ideal gas law as:

$$m = \frac{x_1 V}{r x_2} \quad (11)$$

The cylinder pressure x_1 is a known measurement but it is necessary to estimate the cylinder temperature x_2 from (10) to deduce the mass using (11).

IV. HIGH GAIN OBSERVER STRUCTURE

Consider a system with an additive triangular nonlinearity form that writes as:

$$\begin{aligned} \dot{x} &= A_0 x + \phi(x, u) \\ y &= C_0 x \end{aligned} \quad (12)$$

where

$$A_0 = \begin{bmatrix} 0 & 1 & 0 \\ 0 & \dots & 1 \\ 0 & 0 & 0 \end{bmatrix}, \quad C_0 = [1 \ 0 \ \dots 0] \quad (13)$$

The nonlinear observer is designed according to the following theorem.

Theorem 1 [16]. If $\phi(x, u)$ is globally Lipschitz in x and u and such that $\partial\phi_i(x, u)/\partial x_j = 0$, for $j \geq i+1, 1 \leq i, j \leq n$, then the system (12) admits an observer of the form:

$$\dot{\hat{x}} = A_0\hat{x} + \phi(\hat{x}, u) + \Lambda K_0(C_0\hat{x} - y) \quad (14)$$

where

$$\Lambda = \begin{bmatrix} \lambda & 0 & 0 \\ 0 & \dots & \\ 0 & 0 & \lambda_n \end{bmatrix} \quad (15)$$

with K_0 such that $A_0 - K_0C_0$ is stable and $\lambda, \dots, \lambda_n$ large enough.

The idea of this observer is to use the uniform observability to weight a gain based on the linear part, in order to make the linear dynamics of the observer error dominating the non linear one [17]. The stability of the observer is analyzed next.

a) Stability Analysis: To prove stability, the auxiliary variable $z = \Lambda^{-1}x$ is introduced. When Λ is chosen as $\lambda_2 = \lambda^2, \lambda_3 = \lambda^3, \dots, \lambda_n = \lambda^n$, and considering the triangular structure of (13) and the fact that $C_0 = [1 \ 0 \ \dots 0]$, the error $\epsilon = z - \hat{z}$ dynamics is:

$$\dot{\epsilon} = \lambda(A_0 - K_0C_0)\epsilon + \Lambda^{-1}\delta\epsilon \quad (16)$$

Given the Lyapunov function $V = \epsilon^T P \epsilon$, where P is symmetric and $P > 0$, the following stability condition must be satisfied to guarantee that the error ϵ converges to 0:

$$\lambda\epsilon^T[(A_0 - K_0C_0)^T P + P(A_0 - K_0C_0)]\epsilon + 2\epsilon^T P \Lambda^{-1}(\phi(z) - \phi(\hat{z})) < 0 \quad (17)$$

As it was stated in *Theorem 1*, $\phi(z)$ is Lipschitz, thus $\|\phi(z) - \phi(\hat{z})\| < \delta\|z - \hat{z}\|$ and condition (17) becomes:

$$\lambda\epsilon^T[(A_0 - K_0C_0)^T P + P(A_0 - K_0C_0)]\epsilon + 2\epsilon^T P \Lambda^{-1}\delta\epsilon < 0 \quad (18)$$

K_0 is chosen such that $A_0 - K_0C_0 < -\alpha_v\|e\|^2$, where α_v is a positive constant. Bounding the last term on the left of (18) using $\lambda^{-1}\delta\epsilon < \frac{\beta}{\lambda_{max}(P)}\|\epsilon\|^2$, (λ_{max} denotes the maximum eigenvalue) where $\beta > 0$ is a tuning parameter depending on $\phi(z)$, it yields:

$$\lambda\epsilon^T[(A_0 - K_0C_0)^T P + P(A_0 - K_0C_0)]\epsilon + 2\delta\epsilon^T P \Lambda^{-1}\epsilon < -\lambda\alpha\|\epsilon\|^2 + \frac{\beta}{\text{eig}_{max}(P)}\|\epsilon\|^2 \quad (19)$$

for some constant values $\alpha > 0$. Taking $\lambda > \frac{\beta}{\lambda_{max}(P)\alpha}$ is sufficient to guarantee (19).

V. HIGH GAIN NONLINEAR OBSERVER APPLICATION

In order to use a high gain nonlinear observer like (14) for system (10), the state space system must be transformed to fit the triangular additive form structure of system (12). An equivalent transformation is performed to obtain this result.

Definition 1. A system described by:

$$\dot{x} = f(x, u) = f_u(x), \quad y = h(x) \quad (20)$$

for all $x \in R^n, u \in R^m, y \in R^p$ is said equivalent to the system

$$\dot{z} = F(z, u) = F_u(z), \quad y = H(z) \quad (21)$$

If there exists a diffeomorphism $z = \Phi(x)$ defined on R^n such that:

$$\forall u \in R^m, \frac{\partial\Phi}{\partial x}f_u(x)|_{x=\Phi^{-1}(z)} = F_u(z) \text{ and } h \circ \Phi^{-1} = H$$

System (20) and system (21) are said to be equivalent by $z = \Phi^{-1}$ and if an observer o_2 is an observer for (21) then o_2 is as well an observer for (20)[16]. \diamond

Using this definition, the following equivalence transformation for system (10) is performed:

$$z = [x_1, a_4k_1x_1x_2]^T \quad (22)$$

giving the following system:

$$\begin{bmatrix} \dot{z}_1 \\ \dot{z}_2 \end{bmatrix} = \begin{bmatrix} 0 & 1 \\ 0 & 0 \end{bmatrix} \begin{bmatrix} z_1 \\ z_2 \end{bmatrix} + \phi(z) \quad (23)$$

where

$$\phi(z) = \begin{bmatrix} (a_1 - a_4k_0T_w)z_1 - a_2Q_{h_{comb}} \\ \left(\frac{a_4}{a_4} + a_3 - a_1 - 2a_4k_0T_w\right)z_2 + 2\frac{z_2^2}{z_1} - \\ 2a_2Q_{h_{comb}}\frac{z_2^2}{z_1} \end{bmatrix} \quad (24)$$

System (23) is in triangular additive form and it admits an observer of the form (14). Besides it has been verified that the transformation (22) fulfills the conditions in Definition 1. It is consequently possible to implement a high gain nonlinear observer to estimate z_2 using the known measurement $z_1 = x_1 = p$:

$$\dot{\hat{z}} = A_0\hat{z} + \phi(\hat{z}, u) + \begin{bmatrix} \lambda_1 & 0 \\ 0 & \lambda_2 \end{bmatrix} K_0(C_0\hat{z} - z_1) \quad (25)$$

The linear dynamics is represented in the gain K_0 , deduced from a Kalman filter [18] to ensure the stability of

$A_0 - K_0 C_0$ as it is required for the high gain observer. The parameters λ_1 and λ_2 are chosen large enough to guarantee the system convergence.

To recover the original state space variables of system (10), the inverse of the transformation (22) is performed and provides the states:

$$\hat{x}_1 = \hat{z}_1, \quad \hat{x}_2 = \frac{\hat{z}_2}{a_4 k_1 \hat{z}_1} \quad (26)$$

A. Simulation results

Using the gases law in (11), the enclosed mass is obtained as:

$$\hat{m} = \frac{\hat{x}_1 V}{r \hat{x}_2} \quad (27)$$

Figures 3, 4 and 5 show the results for the operating conditions $N = 2000$ rpm and $IMEP = 10$ bar. Figures 3 and 4 show the cylinder pressure and the temperature estimations during the compression and combustion strokes when the valves are closed. Figure 5 shows an augmented view of the mass estimation to better observe the transitory stabilization. The second simulation case is shown in Figures 6, 7 and 8 where the operating conditions are changed to $N = 4000$ rpm and $IMEP = 1.02$ bar.

The virtual engine model is presented in solid line and the estimation is presented in dashed lines. The estimation appears cut between two bars in the extremes because the observer is valid only when the valves are closed. In the remaining parts of the cycle the observer is disabled and reset. One combustion cycle is enough to accurately observe the variables of interest \hat{x}_1 and \hat{x}_2 .

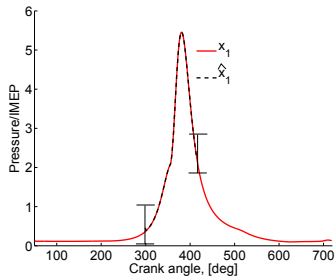


Fig. 3: Case 1: cylinder pressure estimation, $N = 2000$ rpm $IMEP = 10$ bar, $IT = 355$ CA.

B. Simulation analysis

The simulation shows satisfactory results of the enclosed mass estimation during the compression and combustion strokes when the valves are closed. One engine cycle is enough for the observer convergence.

The valves closure has a limited occurrence during the whole engine cycle, consequently limiting the available time for estimation. In this work, the interest is to compute

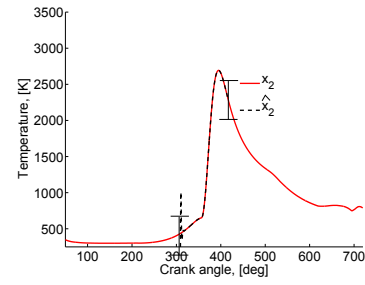


Fig. 4: Case 1: cylinder temperature estimation, $N = 2000$ rpm $IMEP = 10$ bar, $IT = 355$ CA

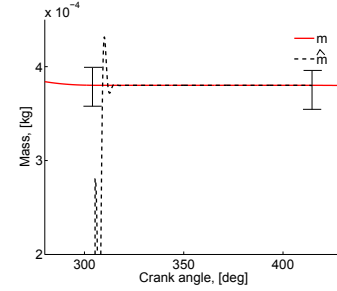


Fig. 5: Case 1: cylinder mass estimation, $N = 2000$ rpm $IMEP = 10$ bar, $IT = 355$ CA

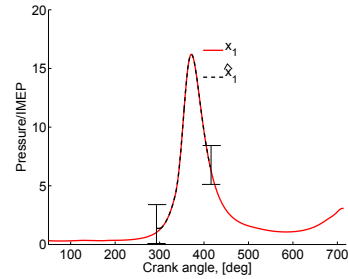


Fig. 6: Case 2: cylinder pressure estimation, $N = 4000$ rpm $IMEP = 1.02$ bar, $IT = 335$ CA

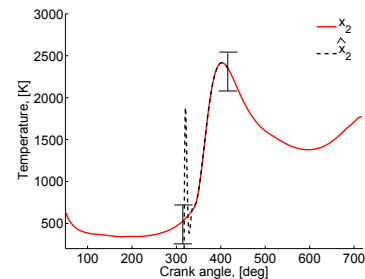


Fig. 7: Case 2: cylinder temperature estimation, $N = 4000$ rpm $IMEP = 1.02$ bar, $IT = 335$ CA

the enclosed mass before the valves opening. Even if the transient behavior of the observation presents an elevated overestimation, the observation is stabilized soon enough before the engine valves opening. The mass estimation is achieved thus before the ignition timing in most operating conditions and the combustion modeling would not be necessary. It might not be the case at high engine speed conditions (4500 rpm up to 5500 rpm), where the

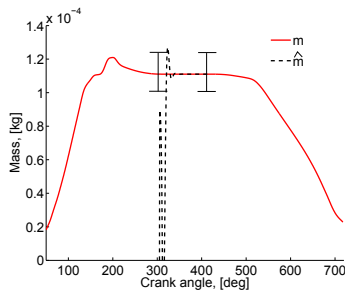


Fig. 8: Case 2: cylinder mass estimation, $N = 4000$ rpm
 $IMEP = 1.02$ bar, $IT = 335$ CA

compression stroke might be too short. For this reason, the estimation algorithm is computed during the compression and combustion strokes. The observer settling time is 0.1 ms. At 1200 rpm the valves closure lasts around 0.68 ms, at 5500 rpm the valves closure lasts 0.145 ms.

The simulation time step is 50 μ s. For this reason, the current work might only be used for benchmark purposes. The adaptation of a similar strategy to be used in the engine control unit will be considered in future research.

VI. CONCLUSION

This work presents a new method to estimate the cylinder enclosed mass during the combustion and compression strokes when the engine valves are closed. A high gain non linear observer of the cylinder temperature during the valves closure is built and the enclosed mass is computed using the observed temperature and the cylinder pressure measurement through the ideal gases law. This approach has shown to be effective to handle the strong non linearities of a combustion model. One engine cycle computation is enough to obtain the mass estimation.

REFERENCES

- [1] Q. Butt and A. Bhatti, "Estimation of gasoline engine parameters using high order sliding mode," *IEEE transactions on industrial electronics*, Vol 55, pages 3891-3898, pp. 3891-3898, 2008.
- [2] M. Muller, "Estimation and control of turbocharged engines," *2008 SAE World Congress Detroit, Michigan*, no. 2008-01-1013, 2008.
- [3] J. Kang and C. Chang, "Observer design for fuel reforming in HCCI engines using a UEGO sensor," *The Engineering Meetings Board*, no. 2009-01-1132, 2009.
- [4] P. Senecal, J. Xin, and R. Reitz, "Predictions of residual gas fraction in IC engines," *Modeling and Diagnostics in Diesel Engines*, SAE, no. 962052, 1996.
- [5] J. Fox, W. Cheng, and J. Heywood, "A model for predicting residual gas fraction in spark-ignition engines," *SAE*, no. 931025, 1993.
- [6] M. Mladek and C. Onder, "A model for the estimation of inducted air mass and the residual gas fraction using cylinder pressure measurement," *Modeling of SI Engines*, no. 2000-01-0958, 2000.
- [7] T. Leroy, G. Alix, J. Chauvin, A. Duarchy, and A. L. Berr, "Modeling fresh air charge and residual gas fraction on dual independent variable valve timing si engine," *SAE Int.J.Engines*, no. 2008-01-0983, 2008.
- [8] M. Hart, M. Ziegler, and O. Loffeld, "Adaptive estimation of cylinder air mass using the combustion pressure," *Electronic engine controls 1998: Diagnostics and Control*, no. 980791, 1998.
- [9] G. Colin, P. Giansetti, Y. Chamaillard, and P. Higelin, "In cylinder mass estimation using cylinder pressure," *SAE*, no. 2007-24-0049, 2007.

- [10] A. Stotsky and S. Eriksson, "Adaptive learning engine load estimation," *Proceedings of the 41st IEEE Conference on Decision and Control*, Las Vegas, 2002.
- [11] H. Kerkeni, J. Lauber, and T. Guerra, "Estimation of individual in-cylinder air mass flow via periodic observer in Takagi-Sugeno form," *Vehicle Power and Propulsion Conference (VPPC)*, Lille, IEEE, 2010.
- [12] M. Rivas, O. Sename, E. Witrant, P. Higelin, and C. Caillol, "Energy wall losses estimation of a gasoline engine using a sliding mode observer," *World congress proceedings, SAE Detroit Conference*, no. 2012-01-0674, 2012.
- [13] G. Woschni, "A universally applicable equation for the instantaneous heat transfer coefficient in the internal combustion engine," *SAE*, no. 670931, 1967.
- [14] J. Meyer, "Engine modeling of an internal combustion engine with twin independent cam phasing," The Ohio State University, Tech. Rep., 2007.
- [15] M. Rivas, P. Higelin, C. Caillol, O. Sename, E. Witrant, and V. Talon, "Validation and application of a new 0d flame/wall interaction sub model for si engines," *Power trains and fuels proceedings, JSAE Kyoto Conference*, no. 2011-01-1893, 2011.
- [16] G. Besancon, *Nonlinear Observer and Applications*. Springer, 2007.
- [17] L. Ljung, *System identification, theory for the user (2nd Ed.)*. Prentice Hall, 1999.
- [18] D. S. Naidu, *Optimal Control Systems*. CRC Press, 2003.

NOMENCLATURE

- α, C_1, C_2 : Calibration constants
 ω_e : Engine speed (rad/s)
 θ : Crank angle degree (rad)
 A_w : Heat transfer wall area
 $IMEP$: Mean effective pressure (bar)
 CAD : Crank angle degrees
 c_v : Specific heat at constant volume
 D : Cylinder bore
 EVC, EVO : Exhaust Valve Closure, Opening
 h : Enthalpy
 h_c : Heat transfer coefficient for wall losses
 H_p : Piston height
 IVC, IVO : Inlet Valve Closure, Opening
 IT : Ignition timing
 k_0, k_1 : Calibration constants
 N : Engine speed (rpm)
 m : Total mass in the combustion chamber
 m_0 : Fuel mass
 p : Pressure
 Q_{th} : Wall losses
 r : Specific gases constant
 T : Temperature
 T_w : Wall temperature
 V : Cylinder volume